# THE DIFFRACTION OF LIGHT BY A CIRCULAR OPENING AND THE LOMMEL WAVE THEORY

By Mason E. Hufford and Harold T. Davis

Abstract

The purpose of this paper is to check the energy in a diffraction pattern of 70 rings secured by passing monochromatc light through a circular orifice. The assumptions made are those of the classical wave theory of light and the mathematical development follows that given in the celebrated papers of E. Lommel. The mathematical interest centers in the discovery of divergent series asymptotic to the Lommel functions $U_1(x)$ and $U_2(x)$.

Photographs of diffraction patterns by circular openings 1.492 cm and 1.832 cm respectively in radius are shown. The smaller of these was used for a comparison of the radii of the diffraction rings calculated by the equations of Lommel's theory with radii measured from the pattern. Graphs of the functions, $M^2$, $J_1$, $U_2$, $U_1$ are shown. Values of these functions were calculated for 256 values of $x$ where $x$ represents the root values of $J_1(x)=0$ and $J_0(x)=0$. The comparison of measured and calculated radii is shown in a table with the percent of difference. The agreement is also shown by a graph. The striking agreement of the calculated energy with that found in the diffraction pattern, particularly as shown in the broadening and darkening of the rings toward the outer part of the pattern, gives renewed confidence in the classical theory of light as applied to diffraction phenomena.

## Introduction

A FEW years ago any problem that had as its aim a checking of the wave theory of diffraction would have been regarded as academic. But the impasse to which the theory of light has been brought by the discovery of the phenomena underlying quantum mechanics has made it again desirable to see how far the interference theory of diffraction, particularly as it has been developed in the classical memoirs of E. Lommel,[1] is in agreement with experiment. With this in mind Professor Hufford secured through a circular orifice the diffraction patterns reproduced in Figures 1 and 2. The large number of rings and the broadening and darkening of the bands toward the outer part of the pattern afforded excellent phenomena to be used in the check of the Lommel theory. Because of the slow convergence of the series expansion of the Lommel functions employed in the calculation of the distribution of energy in the pattern it was found necessary to look for a divergent series which would furnish an asymptotic representation of the functions. This mathematical investigation is contributed by Professor Davis.

Because of the long range over which the energy distribution was calculated existing tables for the roots of the Bessel functions $J_0(x)$ and $J_1(x)$ with the corresponding values of $J_1(x)$ and $J_0(x)$ were extended from

[1] E. Lommel, Abh. der K. Bayer. Akad. der Wissen. **15**, 233–531 (1884–1886).

40 roots to 150 in the one case and from 50 roots to 150 in the second.[2] A contribution from the funds of the Waterman Institute of Indiana University made these calculations possible. Two independent computations of the energy were made and the work was further checked by an independent calculation of the square of the intensity at the root values of $U_2(x)$ which were positions of maximum or minimum energy.[3]

The particularly noteworthy feature of this investigation is the close agreement of experiment and theory. The rings, as is obvious from the energy diagram, Figure 3, ($A$), broaden and become darker toward the outer part of the plate.

## Computation of the Energy [4]

If a monochromatic beam of light of wave-length $\lambda$ and period $T$ propagated in spherical waves from a point source $A$, is allowed to pass through a small circular orifice of radius $r$, it can be shown that the intensity of illumination at a point $P$ on a screen perpendicular to the axis of the beam is proportional to the square root of

$$I^2 = \frac{1}{a^2 b^2 \lambda^2}(C^2+S^2),$$

in which we abbreviate,

$$C = \int_0^{2\pi}\int_0^r \cos\frac{2\pi}{\lambda}\left\{(a+b)\rho^2/2ab - \zeta\rho\cos\phi/b\right\}\rho\, d\rho\, d\theta,$$

$$S = \int_0^{2\pi}\int_0^r \sin\frac{2\pi}{\lambda}\left\{(a+b)\rho^2/2ab - \zeta\rho\cos\phi/b\right\}\rho\, d\rho\, d\theta,$$

where $a$ is the distance of $A$ from the edge of the orifice, $b$ the distance of the screen from the nearest point or pole of the spherical wave, and $\zeta$, the distance of $P$ from the axis of symmetry. The only assumption made in this formula is that the radius is sufficiently small and $P$ sufficiently near the axis so that we may use $b$ for the distance from any element of the wave front in the orifice to $P$.

Our point of departure is from the square of Lommel's expression for the intensity of illumination at a point $x$ from the axis of symmetry, which is proportional to

$$M^2 = U_1{}^2 + U_2{}^2, \tag{1}$$

in which we abbreviate,

$$U_1(x) = \sin \tfrac{1}{2} y^2(1+\omega^2) - V_1(x), \tag{2}$$

$$U_2(x) = -\cos \tfrac{1}{2} y^2(1+\omega^2) + V_0(x), \tag{3}$$

[2] A new Table of the Zeros of the Bessel Functions, H. T. Davis and W. J. Kirkham, Bull. Amer. Math. Soc. **33**, pp. 760–772 (1927).

[3] This computation was greatly assisted by W. J. Kirkham and V. V. Latshaw.

[4] See Gray, Mathews and MacRobert, Bessel Functions, MacMillan (1922), Chapter XIV.

$$V_0(x)=J_0(x)-\omega^2 J_2(x)+\omega^4 J_4(x)-\cdots \tag{4}$$

$$V_1(x)=\omega J_1(x)-\omega^3 J_3(x)+\omega^5 J_5(x)-\cdots \tag{5}$$

where $\omega=x/y$, $y=4\pi r^2(a+b)/2\lambda ab$ and $J_n(x)$ is the Bessel function of first kind of order $n$. The series defining $V_0$ and $V_1$ are clearly convergent since $\lim_{n=\infty} J(x)_{n+2}/J(x)_n=\lim_{n=\infty} x^2/4(n+1)(n+2)=0$, but the convergence for comparatively large values of $x$ becomes exceedingly slow and tables of $J_n(x)$ are not available beyond $x=24$ when $n>1$.

In view of the fact that we have

$$\frac{\partial M^2}{\partial x}=-2\left(\frac{2}{y}\right)^2 J_1(x)\,U_2(x),$$

from which it appears that maximum and minimum values of the energy occur at the roots of $J_1(x)=0$ and $U_2(x)=0$, it is clearly desirable to evaluate $V_0(x)$ and $V_1(x)$ at the root values of the first equation, which we designate by $x_1^{(S)}$, where $S$ is the number of the root. Since it is also desirable to interpolate values at stations between $x_1^{(S+1)}$, and $x_1^{(S)}$, we shall also compute $V_0(x)$ and $V_1(x)$ at the zeros of $J_0(x)$, designating these values by $x_0$. It thus becomes convenient to express $V_0(x)$ and $V_1(x)$ in terms of $J_0(x)$ and $J_1(x)$. This is accomplished by means of the series:[2]

$$\begin{aligned}J_{2n}(x)=(-1)^n&\left[1+\sum_{r=1}^{n-1}(-1)^r\frac{2^{2r}n^2(n^2-1)^2\cdots[n^2-(r-1)^2]^2(n^2-r^2)}{(2r)!\,x^{2r}}\right]J_0(x)\\&+(-1)^{n+1}\left[\sum_{r=0}^{n-1}(-1)^r\frac{2^{2r+1}n^2(n^2-1)^2(n^2-4)^2\cdots(n^2-r^2)^2}{(2r+1)!\,x^{2r+1}}\right]J_1(x).\end{aligned} \tag{6}$$

$$\begin{aligned}J_{2n-1}(x)=(-1)^{n+1}&\left[\sum_{r=0}^{n-2}(-1)^r\frac{2^{2r+1}n^2(n^2-1)^2\cdots[n^2-(r-1)^2]^2(n^2-r^2)(n-r)(n-r-1)}{(2r+1)!\,x^{2r+1}}\right]J_0(x)\\&+(-1)^{n+1}\left[1+\sum_{r=1}^{n-1}(-1)^r\frac{2^{2r}n^2(n^2-1)^2\cdots[n^2-(r-1)^2]^2(n-r)^2}{(2r)!\,x^{2r}}\right]J_1(x)\end{aligned} \tag{7}$$

Substituting (6) in (4) and (7) in (5) we get,

$$\begin{aligned}V_0(x)&=\sum_{n=0}^{\infty}(-1)^n\omega^{2n}J_{2n}(x),\\&=\sum_{n=0}^{\infty}\omega^{2n}[1-2^2n^2(n^2-1)/2!x^2+2^4n^2(n^2-1)^2(n^2-4)/4!x^4-\cdots]J_0(x)\\&-\sum_{n=0}^{\infty}\omega^{2n}[2n^2/x-2^3n^2(n^2-1)^2/3!x^3+2^5n^2(n^2-1)^2(n^2-4)^2/5!x^5-\cdots]J_1(x)\end{aligned} \tag{8}$$

$$\begin{aligned}V_1(x)&=\sum_{n=1}^{\infty}(-1)^{n+1}\omega^{2n-1}J_{2n-1}(x),\\&=\sum_{n=1}^{\infty}\omega^{2n-1}[2n(n-1)/x-2^3n^2(n^2-1)(n-1)(n-2)/3!x^3\\&\qquad+2^5n^2(n^2-1)^2(n^2-4)(n-2)(n-3)/5!x^5\cdot-\cdots]J_0(x)\\&+\sum_{n=1}^{\infty}\omega^{2nr}[1-2^2n^2(n-1)^2/2!x^2+2^4n^2(n^2-1)^2(n-2)^2/4!x^4-\cdots]J_1(x).\end{aligned} \tag{9}$$

Defining a new function,

$$S_m(x) = \sum_{n=1}^{\infty} n^m x^n,$$

we see that $S_m(x)$ can be evaluated for any subscript from the relations:

$$S_0(x) = x/(1-x), \qquad S_{m+1}(x) = x\frac{d}{dx}S_m(x).$$

Making use of the formulas thus obtained we can evaluate the sums in (8) and (9). For example,

$$\sum_{n=o}^{\infty} \omega^{2n}n^2(n^2-1) = S_4(\omega^2) - S_2(\omega^2) = 12(\omega^4+\omega^6)/(1-\omega^2)^5.$$

We thus derive the following asymptotic series:

$$V_0(x) \sim \left\{\frac{1}{1-\omega^2} - \frac{24\omega^4(1+\omega^2)}{x^2(1-\omega^2)^5} + \frac{1920\omega^6(1+6\omega^2+6\omega^4+\omega^6)}{x^4(1-\omega^2)^9} - \cdots\right\} J_0(x)$$
$$- \left\{\frac{2\omega^2(1+\omega^2)}{x(1-\omega^2)^3} - \frac{48\omega^4(1+9\omega^2+9\omega^4+\omega^6)}{x^3(1-\omega^2)^7} + \frac{3840(1+25\omega^2+100\omega^4+100\omega^6+25\omega^8+\omega^{10})}{x^5(1-\omega^2)^{11}} - \cdots\right\} J_1(x)$$

$$V_1(x) \sim \left\{\frac{4\omega^3}{x(1-\omega^2)^3} - \frac{192\omega^5(1+3\omega^2+\omega^4)}{x^3(1-\omega^2)^7} + \frac{23040\omega^7(1+10\omega^2+20\omega^4+10\omega^6+\omega^8)}{x^5(1-\omega^2)^{11}} - \cdots\right\} J_0(x)$$
$$+ \left\{\frac{\omega}{1-\omega^2} - \frac{8\omega^3(1+4\omega^2+\omega^4)}{x^2(1-\omega^2)^5} + \frac{384\omega^5(1+16\omega^2+36\omega^4+16\omega^6+\omega^8)}{x^4(1-\omega^2)^9} - \cdots\right\} J_1(x).$$

It is beyond the scope of this paper to discuss the asymptotic character of these series. They are unusual, however, in the range to which they apply. For small values of $x$ their convergence is accelerated by the smallness of $\omega^2$ and for small values of $1-\omega^2$ convergence is secured through large values of $x$. In the calculations of the present paper, $y=443.87$ and the range of $x$ is from 0 to 400. For $x=24$, $\omega^2=0.0029$ the series converges to $V_0(x)$ with an error not greater than $42\times10^{-10}$. For $x=393.48$ and $\omega^2=0.7859$ the error does not exceed 0.006 which is well within the error of the experiment.

In checking the energy diagram the values of $M^2$ were also calculated at each of the 57 roots of $U_2(x)=0$. These roots and the corresponding values of $V_0(x)$ and $V_1(x)$ were calculated by interpolation.

## Experimental

In a previous paper[5] some experiments were described in which diffraction patterns were produced by light diffracted about spherical objects. The theory of Lommel for this type of diffraction was verified for the range presented by the experiment. The diffraction patterns shown in this paper are those in which monochromatic light passed through circular openings. These patterns are unusually large for this type of diffraction and offer therefore an opportunity to verify the Lommel theory for this case through a wider range than has been possible before. In Lommel's original paper is contained a description of a check of theory by experiment in which he produced a system of five microscopic rings through a needle hole in paper.

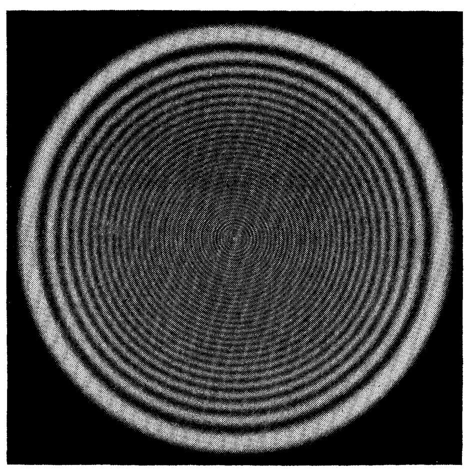

Fig. 1. Diffraction pattern, opening 1.492 cm.

The agreement through that short range was very satisfactory. Figure 1 of the patterns here shown was selected for the purpose of verification and Figure 2 is included because of the large number of diffraction rings which it contains.

For the purpose of producing these diffraction patterns apparatus similar to that described in a previous paper[6] was arranged. Figure 1 was obtained by light through an opening 1.492 cm in radius and Figure 2 by an opening 3.664 cm in radius. These openings made in lead plates were mounted at a distance $a=1552$ cm from a light source 0.022 cm in diameter. The distance from the diffracting object to the receiving screen was $b=1706$ cm. The edges of the openings were polished smooth. Monochromatic light of wave-length 3880A was isolated from the carbon spectrum and passed through the hole at the source. The exposure was for three hours. By the conditions of the experiment, the value of $y$ in the Lommel equations becomes $y=443.87$.

[5] Hufford, Phys. Rev. **7**, 545 (1916).
[6] Hufford, Phys. Rev. **3**, 241 (1914).

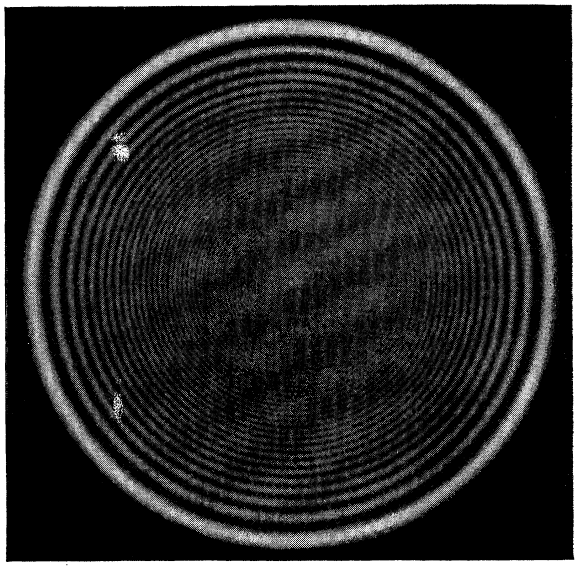

Fig. 2. Diffraction pattern, opening 3.664 cm.

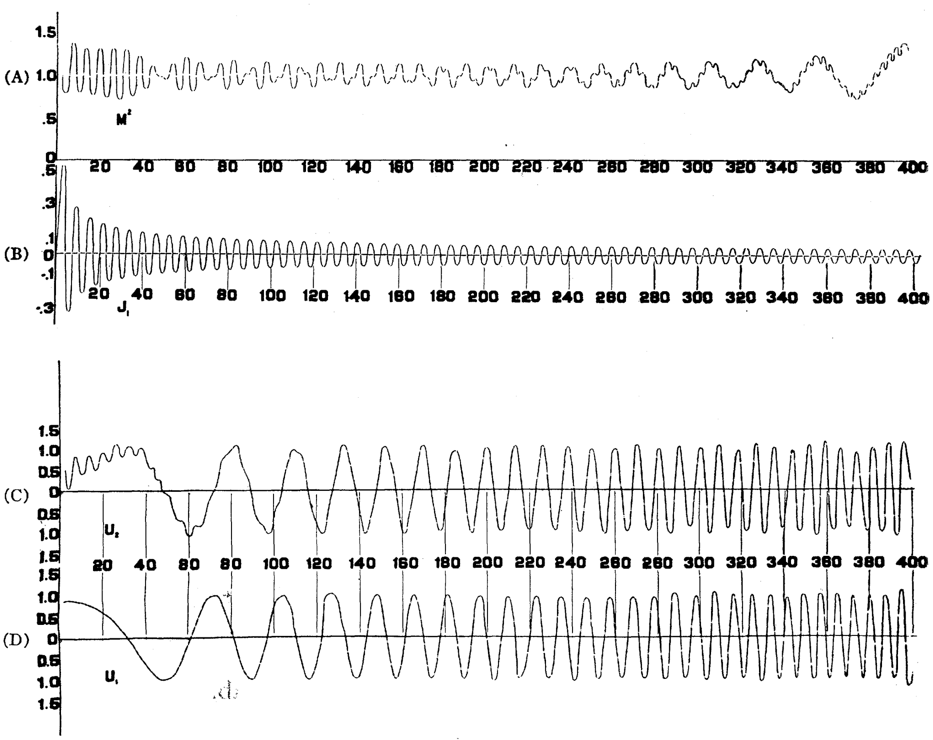


Fig. 3. Graphs of functions $M^2$, $J_1$, $U_2$ and $U_1$.

The values of $U_1(x)$ and $U_2(x)$ for this pattern have been calculated using values of $x$ corresponding to the roots of $J_1(x)=0$ and $J_0(x)=0$, by the use of the asymptotic series $V_0(x)$ and $V_1(x)$ substituted in equations (2) and (3). Each of the calculations involved in obtaining values for the terms of the coefficients of $J_0(x)$ and $J_1(x)$ were made separately by each of us and results were checked. The graphs $U_1(x)$ and $U_2(x)$ were plotted throughout the range of the pattern of Figure 1 at the values of $x$ corresponding to the roots of $J_0(x)=0$ and $J_1(x)=0$. These graphs are shown in Fig. 3 $C$ and $D$. It is the sum of the squares of the ordinates of these graphs which give $M^2$ proportional to the energy. The value of $M^2$ plotted as ordinates at the same values of $x$ as used in the graphs mentioned gives the energy curve. This curve is shown in Fig. 3 $A$. From this graph of intensity, maxima and minima of light energy in the diffraction pattern are clearly

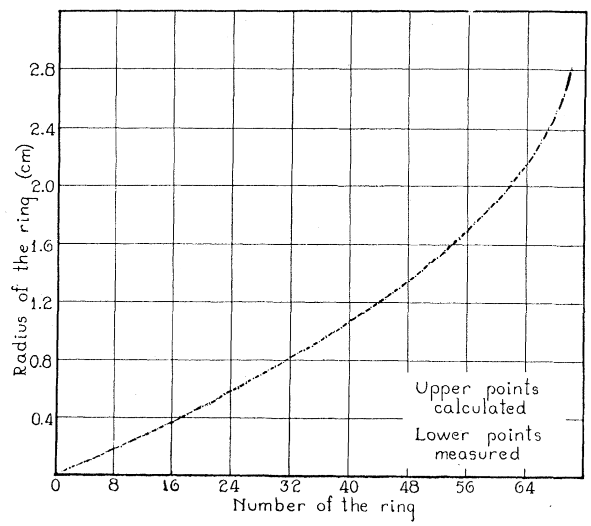


Fig. 4. Graphical comparison of the theoretical and experimental values of the radii of the diffraction rings.

indicated. It will be observed that secondary maxima and minima are shown. It was impossible to detect these on the photographic plate due to the failure of the plate in showing such small differences in intensity.

Since the roots of $J_1(x)=0$ as well as those of $U_2(x)=0$ are critical values for maxima and minima, the graph of $J_1(x)$ is also shown in Fig. 3 $B$.

In order to compare theory with experiment, the values of $x$ for maxima and minima were read from the graph of $M^2$. These were substituted in Lommel's equation, $\zeta = b\lambda x/2\pi r$ where $\zeta$ is the radius of the bright or dark diffraction ring and $r$ is the radius of the diffracting opening. The radii of the bright and dark rings of the pattern in Fig. 1 were measured by micrometer microscope from the photographic plate. Table I includes the averages of ten independent measurements of the rings and the radii as computed from Lommel's equation. The percent of difference is also given.

The agreement is also represented graphically in Fig. 4. It will be observed in the energy diagram, Fig. 3 *A*, that at the fifteenth ring and again at the twenty first, there is a change in the intensity as compared to the adjacent dark rings. It was hoped that sufficient refinement could be developed in the experiment to show this difference. However all the diffraction photographs fail to show the effect, to any degree of certainty. The failure is probably accounted for by the small difference in intensity between these rings and the dark rings on either side. At no place do the dark rings represent a total absence of light. The graph Fig. 3 *A* shows that the dark rings have approximately two thirds the intensity of the bright rings. However in the outer rings the difference becomes greater as the theory predicts and experiment confirms. From the graph Fig. 3 *A*, the fifteenth and twenty first rings are approximately eighty five percent as intense as the adjacent bright rings and only about twenty percent brighter than the dark rings of the region. The photographic plates used did not show this small difference.

TABLE I. *Observed and calculated radii of diffraction rings* $y=443.87$; $r=1.492$ *cm.*

| No. | Intensity | $\chi$ for $J_1(\chi)=0$ or $U_2(\chi)=0$ | Radius (calc.) | Radius (obs.) | Per cent diff. | No. | Intensity | $\chi$ for $J_1(\chi)=0$ or $U_2(\chi)=0$ | Radius (calc.) | Radius (obs.) | Per cent diff. |
|---|---|---|---|---|---|---|---|---|---|---|---|
| 1 | D | J | 0.0271 | 0.0294 | 8.0 | 36 | B | J | 0.9372 | 0.9345 | 0.3 |
| 2 | B | J | 0.0495 | 0.0482 | 3.0 | 37 | D | U | 0.9594 | 0.9685 | 1.0 |
| 3 | D | J | 0.0718 | 0.0740 | 3.0 | 38 | B | J | 1.0047 | 0.9986 | 0.6 |
| 4 | B | J | 0.0941 | 0.0938 | 0.3 | 39 | D | J | 1.0259 | 1.0323 | 0.6 |
| 5 | D | J | 0.1163 | 0.1189 | 2.0 | 40 | B | J | 1.0703 | 1.0624 | 0.7 |
| 6 | B | J | 0.1385 | 0.1399 | 0.3 | 41 | D | J | 1.0924 | 1.0988 | 0.6 |
| 7 | D | J | 0.1607 | 0.1653 | 3.0 | 42 | B | J | 1.1368 | 1.1313 | 0.5 |
| 8 | B | J | 0.1829 | 0.1852 | 1.0 | 43 | D | U | 1.1692 | 1.1676 | 0.1 |
| 9 | D | J | 0.2051 | 0.2103 | 2.0 | 44 | B | J | 1.2033 | 1.2029 | 0.0 |
| 10 | B | J | 0.2273 | 0.2303 | 1.0 | 45 | D | J | 1.2255 | 1.2399 | 1.0 |
| 11 | D | J | 0.2495 | 0.2549 | 2.0 | 46 | B | U | 1.2815 | 1.2763 | 0.5 |
| 12 | B | J | 0.2717 | 0.2758 | 2.0 | 47 | D | J | 1.3143 | 1.3160 | 0.1 |
| 13 | D | J | 0.2939 | 0.3005 | 2.0 | 48 | B | J | 1.3586 | 1.3505 | 0.6 |
| 14 | B | J | 0.3160 | 0.3223 | 2.0 | 49 | D | U | 1.3909 | 1.3939 | 0.2 |
| 15 | D | U | 0.3361 | 0.3495 | 4.0 | 50 | B | U | 1.4368 | 1.4319 | 0.4 |
| 16 | B | J | 0.3604 | 0.3759 | 4.0 | 51 | D | U | 1.4849 | 1.4754 | 0.6 |
| 17 | D | J | 0.4048 | 0.4047 | 0.0 | 52 | B | J | 1.5139 | 1.5137 | 0.0 |
| 18 | B | J | 0.4270 | 0.4284 | 3.0 | 53 | D | J | 1.5583 | 1.5602 | 0.1 |
| 19 | D | J | 0.4491 | 0.4532 | 0.9 | 54 | B | J | 1.6026 | 1.6029 | 0.1 |
| 20 | B | J | 0.4713 | 0.4761 | 1.0 | 55 | D | J | 1.6470 | 1.6511 | 0.3 |
| 21 | D | J | 0.4935 | 0.5023 | 2.0 | 56 | B | U | 1.7034 | 1.6973 | 0.4 |
| 22 | B | J | 0.5379 | 0.5303 | 1.0 | 57 | D | J | 1.7580 | 1.7498 | 0.5 |
| 23 | D | J | 0.5601 | 0.5610 | 0.2 | 58 | B | J | 1.8023 | 1.7962 | 0.3 |
| 24 | B | J | 0.5823 | 0.5851 | 0.5 | 59 | D | U | 1.8591 | 1.8543 | 0.3 |
| 25 | D | J | 0.6040 | 0.6127 | 1.0 | 60 | B | J | 1.9132 | 1.9039 | 0.5 |
| 26 | B | J | 0.6488 | 0.6392 | 2.0 | 61 | D | U | 1.9683 | 1.9646 | 0.2 |
| 27 | D | J | 0.6710 | 0.6689 | 0.3 | 62 | B | U | 2.0370 | 2.0239 | 0.6 |
| 28 | B | J | 0.6932 | 0.6963 | 0.5 | 63 | D | U | 2.1034 | 2.0945 | 0.4 |
| 29 | D | U | 0.7350 | 0.7251 | 1.0 | 64 | B | U | 2.1671 | 2.1576 | 0.4 |
| 30 | B | J | 0.7597 | 0.7531 | 1.0 | 65 | D | U | 2.2326 | 2.2387 | 0.3 |
| 31 | D | J | 0.7819 | 0.7843 | 0.3 | 66 | B | U | 2.3244 | 2.3151 | 0.4 |
| 32 | B | U | 0.8198 | 0.8119 | 1.0 | 67 | D | U | 2.4120 | 2.4073 | 0.2 |
| 33 | D | J | 0.8485 | 0.8437 | 0.4 | 68 | B | U | 2.5249 | 2.5121 | 0.5 |
| 34 | B | J | 0.8706 | 0.8732 | 0.3 | 69 | D | J | 2.6452 | 2.6365 | 0.3 |
| 35 | D | U | 0.9010 | 0.9060 | 0.5 | 70 | B | J | 2.8005 | 2.8317 | 1.0 |

As shown in the intensity graph, Fig. 3 *A*, the theory indicates that there is a system of fine fringes superimposed upon the dark and bright rings. These the photographs also fail to show. In accounting for this failure along with that pointed out above it should be mentioned that with a source 0.022 cm in diameter and approximately equal distances from plate and opening on the one side and source and opening on the other, the dark rings should have an increased width equal to the diameter of the source. This would tend to obliterate details as minute as these fringes.

It should be mentioned also that with a source as large as that used here, the light cannot be regarded as strictly monochromatic. This also would tend to smooth out the intensity in the dark rings and obscure the superposed fringes.

Despite the want of these details in the photographs the fact that they verify the theory in respect to the number of rings and their radii and that the rings become more intense and more widely separated in the outer regions is a triumph for the theory presented by Lommel. The photographs are of interest also because of the great number of rings and the large diffraction patterns produced through large distances.

## Conclusion

The diffraction photographs here shown are large patterns for this type of diffraction. The very large number of rings has offered an opportunity for testing the classical wave theory as developed by Lommel for this range. This is of special interest as a wider application of the wave nature of light at a time when the assumption has been challenged by experiments underlying the quantum theory of radiant energy. The agreement obtained between theory and experiment lends new confidence to the wave theory.

Waterman Institute for Research,
Indiana University,
August, 1928.

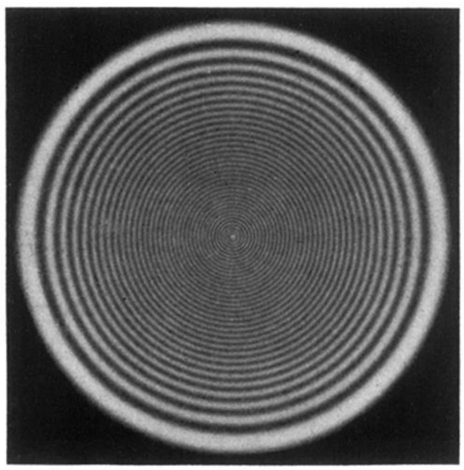

Fig. 1. Diffraction pattern, opening 1.492 cm.

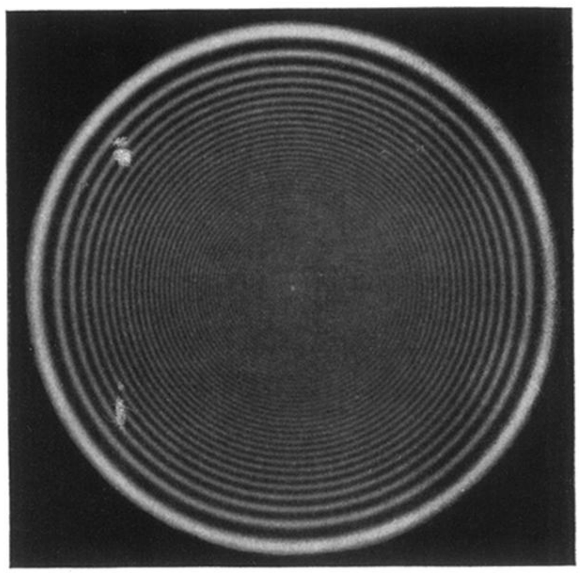

Fig. 2. Diffraction pattern, opening 3.664 cm.